

DEVELOPMENT OF A WIND TURBINE BLADE PROFILE ANALYSIS CODE BASED ON THE SINGULARITIES METHOD

David AFUNGCHUI¹, Badreddine KAMMOUN², Alain CHAUVIN³,
(1 et 2). Faculté des Sciences de Sfax Département de Physique
Labo. de Recherche de Physique Appliquée (L.R.P.A)
BP 802, 3018 Rte Soukra, Km 3,5 Sfax-TUNISIE
Tel: (216)74 276400 Fax: (216)74 274437
1. (E-Mail : afungchui@yahoo.fr)
2. (E-Mail : badre.kamoun@fss.rnu.tn)

3. Université de Provence ;Institut Universitaire des Systèmes Thermiques Industriels (I.U.S.T.I), 5 rue Enrico
Fermi 13453 Marseille Cedex 13, France
(E-Mail : chauvin@polytech.univ-mrs.fr)

ABSTRACT

The quest of renewable energies that preserves the environment is an issue of major importance. Wind energy is one typical example among many others. The aerodynamic characteristics of wind turbines are closely related to the geometry of their blades. The innovation and the technological development of wind turbine blades can be centered on two tendencies. The first is to improve the shape of the existing blades, in order to achieve an optimal circulation. The second is to design new shapes of blades in order to get some more ambitious aerodynamic characteristics.

This paper present an airfoil analysis code achieved by solving the direct problem. The 2D incompressible potential flow model has been used. In the light of the singularities method or Panel method, source-vortex distributions over the airfoil contour are used to compute the flow characteristics. The accuracy and the validity of the results are tested using experimental and numerical results obtained from Wind Turbine Airfoil Catalogue “*Risø National Laboratory, Roskilde, Denmark, August 2001*”.

KEYWORDS: Singularities, incompressible potential flow, Aerodynamics, Lift, drag, pitching moment.

Nomenclature

<p>Z The complex plane</p> <p>Z_i Coordinate of point i on a line segment in the complex plane</p> <p>Z_T Coordinates of the trailing edge</p> <p>x Abscissa of the Cartesian coordinate system</p> <p>y Ordinate of the Cartesian coordinate system</p> <p>S Curvilinear distance on the airfoil contour</p> <p>\hat{x} Unit vector in the x-direction</p> <p>\hat{y} Unit vector in the y-direction</p> <p>\hat{n} Normal unit vector of the local coordinate system linked to the airfoil</p> <p>\hat{s} Tangential unit vector of the local coordinate system linked to the airfoil</p> <p>\vec{V}_0 Free stream velocity</p> <p>w Induced velocity</p> <p>u_s Tangential component of the induced velocity</p>	<p>u_{si} Tangential component of the induced velocity of the i^{th} panel</p> <p>v_n Normal component of the induced velocity</p> <p>q Source strength</p> <p>q_i Source strength on the i^{th} panel</p> <p>Subscripts</p> <p>c Collocation point</p> <p>ex Upper surface of airfoil</p> <p>in lower surface of airfoil</p> <p>Greek Symbol</p> <p>γ Vortex strength</p> <p>Φ Velocity potential</p> <p>Ψ Stream function</p> <p>θ Angular distance between local coordinate system and Cartesian coordinate system</p> <p>α Attack angle at the leading edge of the airfoil</p>
---	---

1. INTRODUCTION

Incompressible inviscid flow is governed by Laplace's equation. An extremely general method to solve this equation is the singularities method.

The complex potential that characterises flow over airfoils can be induced by various distributions of singularities. The choice of the type of singularities to use depends on the boundary conditions imposed. By choosing either the Dirichlet or the Neumann boundary condition, the incompressible and irrotational flow over an airfoil can be treated using either the velocity potential or the stream function. These two quantities joined together constitute the complex potential. The complex potential induced by a segment of a blade profile is a multi-valued function and the correct value has to be taken from an appropriate sheet of the Riemann surfaces. For the analytical formulations of a homogenous density distribution of sources and vortices over a segment of an airfoil contour, the multi-valued part is located at one of the end points of each segment. The computation is structured to get the right definition of the multi-valued function with respect to the relative positions of the induction element and the reception point.

The resolution of the field problem yields the source vortex distributions and the velocity distributions over the contour of the airfoil. The lift forces, drag forces, moments and the pressure distributions are then computed.

2. COMPLEX POTENTIAL OF THE SIMPLE LAYER AND THE INDUCED VELOCITY

In the complex plane z , consider a source and vortex distributions applied on a line segment $[z_1, z_2]$; if the density $(q+i\gamma)$ is constant over each segment, the complex potential induced at a point z is given by [1]:

$$f(z) = \phi + i\psi = \frac{q+i\gamma}{2\pi} e^{-i\theta_0} \left[(z-z_2)(1-\text{Log}(z-z_2)) - (z-z_1)(1-\text{Log}(z-z_1)) \right]$$

We notice the existence of two multiform functions $\text{Log}(z-z_1)$ and $\text{Log}(z-z_2)$. To eliminate one of them, we proceed as follows :

$$\begin{aligned} \phi + i\psi &= \frac{q+i\gamma}{2\pi} e^{-i\theta_0} \left[(z_1-z_2) - (z-z_2)\text{Log}(z-z_2) + (z-z_1-z_2+z_2)\text{Log}(z-z_1) \right] \\ \Leftrightarrow \phi + i\psi &= \frac{q+i\gamma}{2\pi} e^{-i\theta_0} (z_2-z_1) \left[\text{Log}(z-z_1) - 1 + \frac{z-z_2}{z_2-z_1} \text{Log}\left(\frac{z-z_1}{z-z_2}\right) \right] \end{aligned} \quad (\text{I})$$

Where $\theta_0 = \arg(z_2 - z_1)$

Lets pose : $Z_n = z - z_n$, $\eta = \frac{z_2 - z_1}{2}$ and $(z_2 - z_1)e^{-i\theta_0} = \Delta S = |z_2 - z_1|$; where $n=1,2$ then (I) becomes :

$$\phi + i\psi = \frac{q+i\gamma}{2\pi} \Delta S \left[\text{Log} Z_1 - 1 + \frac{Z_2}{2\eta} \text{Log} \frac{Z_1}{Z_2} \right] \quad (\text{II})$$

The function $\text{Log}\left(\frac{Z_1}{Z_2}\right)$, is uniform but discontinuous across the segment $[z_1, z_2]$.

To precise the determination of the multiform function $\text{Log} Z_1$, we effectuate a cut of the Riemann surface along the segment $[z_1, z_2]$ and we prolong the cut to the side of z_1 [4;6]. As we can write : $\text{Log} Z_i = \text{Log}|Z_i| + i\theta_i$, where θ_i is the angle between Z_i and the x -axes, there is no indetermination for ϕ with a distribution of sources q alone, nor for ψ with a distribution of vortices γ alone.

As the potential is defined with respect to a reference value, we can neglect the constant term;

$$-\left(\frac{(q+i\gamma)\Delta S}{2\pi} \right), \text{ in equation (II).}$$

By deriving (II), we obtain the induced velocity on the segment $[z_1, z_2]$ given by:

$$w(z) = \frac{\partial \phi}{\partial x} - i \frac{\partial \phi}{\partial y} = \frac{q + i\gamma \Delta S}{2\pi \cdot 2\eta} \left[\text{Log} \frac{Z_1}{Z_2} \right] \quad (\text{III})$$

In the local coordinate system \vec{s} and \vec{n} in the directions tangential and normal to the segment $[Z_1, Z_2]$ and centered at the point z , (III) is written as:

$$w(z) = \frac{\partial \phi}{\partial s} - i \frac{\partial \phi}{\partial n} = \left(\frac{\partial \phi}{\partial x} - i \frac{\partial \phi}{\partial y} \right) e^{i\theta} = \frac{q + i\gamma \Delta S}{2\pi \cdot 2\alpha} e^{i\theta} \left[\text{Log} \frac{Z_1}{Z_2} \right] = u_s - i v_n \quad (\text{IV})$$

where θ is the angle between the tangential unit vector \vec{s} and the \vec{x} -axis and u_s and v_n are respectively the tangential and normal components of the induced velocity.

3. THE SINGULARITIES METHOD APPLIED TO AIRFOILS

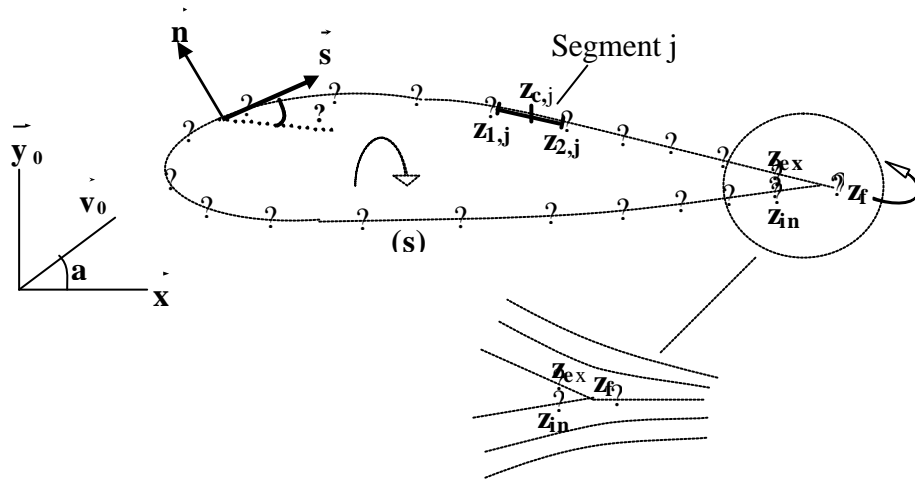


Fig.1

We consider an airfoil of boundary S transverse to the wind direction fig.1. The wind is moving with an unperturbed upstream velocity \vec{V}_0 at an incident angle α . The irrotationality condition is automatically satisfied if the flow field is characterised by the velocity potential ϕ . The relative velocity of the air over the airfoil is given by[3]:

$$\vec{V} = \vec{V}_0 + \nabla \phi \quad (\text{V})$$

The continuity equation leads to the Laplace equation:

$$\nabla^2 \phi = 0 \quad (\text{VI})$$

With the incident angle α defined; \vec{V}_0 is given by :

$$\vec{V}_0 = \cos \alpha \vec{i} + \sin \alpha \vec{j} \quad (\text{VII})$$

On the contour of the airfoil, the tangential unit vector \vec{s} is oriented in the clockwise direction and the unit normal vector \vec{n} is deduced from \vec{s} by a rotation of $\pi/2$.

If θ is the inclination of \vec{s} with respect to the x -axis, then we can write :

$$\vec{s} = \cos \theta \vec{i} + \sin \theta \vec{j} \quad \text{and} \quad \vec{n} = -\sin \theta \vec{i} + \cos \theta \vec{j} \quad (\text{VIII})$$

The slip condition on the airfoil contour can be written :

$$\vec{V} \cdot \vec{n} = 0 \Leftrightarrow (\vec{V}_0 + \nabla \phi) \cdot \vec{n} = 0$$

$$\Leftrightarrow \overrightarrow{\text{grad } \phi} \cdot \overrightarrow{n} = - \overrightarrow{V}_0 \cdot \overrightarrow{n} \quad (\text{IX})$$

$$\Leftrightarrow \frac{d\phi}{dn} = \cos\alpha \sin\theta - \sin\alpha \cos\theta \quad (\text{X})$$

In order to apply this boundary condition, sources are distributed on the airfoil contour ; but in order to produce lift , vortices are also distributed. The source strength is constant over each line segment but has a different value for each segment while the vortex strength is constant and equal over each line segment. The Kutta-Joukowski condition enables us to determine the unknown vortex distribution on the airfoil contour. The Kutta-Joukowski condition states that the flow must leave the trailing edge smoothly. The Kutta condition is satisfied by equating velocity components tangential to the segments adjacent to the trailing edge on the upper and lower sides. This is equivalent to imposing a second stagnation point at the trailing edge Z_T in the case of thick airfoils. Lets consider two points Z_{ex} and Z_{in} situated respectively on the last segments of the upper side and lower side of the airfoil adjacent to the trailing edge with : $|Z_{ex}-Z_T|=|Z_{in}-Z_T|\rightarrow 0$. The Kutta-Joukowski condition at these two points is written from equation (V) as follows:

$$\overrightarrow{V}_0 \cdot \overrightarrow{s}_{ex} + (\phi'_s)_{ex} = - \left(\overrightarrow{V}_0 \cdot \overrightarrow{s}_{in} + (\phi'_s)_{in} \right) \quad (\text{XI})$$

where : $\overrightarrow{V}_0 \cdot \overrightarrow{s} = \cos\theta \cos\alpha + \sin\alpha \sin\theta$

As the potential f is generated by a distribution of sources with variable densities and a homogenous distribution of vortex over the contour S of the blade profile, we can write[3] :

$$\phi = R \left[\int_S \frac{q+i\gamma}{2\pi} \text{Log}(z-z_0) e^{-i\theta_0} dz_0 \right] \quad (\text{XII})$$

where R stands for the real part of the expression, q the source strength, is an unknown function of the curvilinear abscissa S and γ , the vortex strength, is an unknown constant. By combining (IV),(IX) and (XII),the boundary conditions can be written as:

$$-\text{Im} \left[\int_S \frac{q+i\gamma}{2\pi} \frac{e^{-i(\theta-\theta_0)}}{z-z_0} dz_0 \right] = - \overrightarrow{V}_0 \cdot \overrightarrow{n}; \quad \text{for } z \in S \quad (\text{XIII})$$

$$\sum_{z=z_{in} \text{ et } z_{ex}} R \left[\int_S \frac{q+i\gamma}{2\pi} \frac{e^{i(\theta-\theta_0)}}{z-z_0} dz_0 \right] = - \overrightarrow{V}_0 \cdot (\overrightarrow{s}_{in} + \overrightarrow{s}_{ex}) \quad ; \text{ Kutta-Joukowski} \quad (\text{XIV})$$

The contour of the airfoil is discretized in to K ($K \in \mathbb{N}$); line segments following the clockwise direction from the trailing edge of the lower side to the trailing edge of the upper side. The segments are numbered from 1 to K . Let the inductor segment be the i^{th} segment, its extremities are taken to be $(z_1)_i$ and $(z_2)_i$; the collocation point where the boundary conditions are applied is the centre $(z_c)_j$ of the j^{th} receptor segment. The airfoil contour is discretized such that the first and last segments adjacent to the trailing edge Z_T are of the same length .The points Z_{ex} and Z_{in} are merged up respectively with the points $(z_c)_1$ et $(z_c)_k$.

To obtain quality results the node points are smoothly distributed while concentrating points at the trailing and leading edges using the spacing function $y(x)$ whose expression is:

$$y(x) = x - \frac{1}{4\pi} \sin(2\pi x) \quad (\text{XV})$$

At the collocation point of each segment, the tangential direction is taken in the sense $Z_1 Z_2$. From equations (XIII) and (XIV), we can then write the following system of equations for the different collocation points:

$$[A_{ij}] \begin{bmatrix} q_1 \\ q_2 \\ \vdots \\ q_k \\ \gamma \end{bmatrix} = \begin{bmatrix} \vec{V}_0 \cdot \vec{n}_1 \\ \vec{V}_0 \cdot \vec{n}_2 \\ \vdots \\ \vec{V}_0 \cdot \vec{n}_K \\ -\vec{V}_0 \cdot (\vec{s}_1 + \vec{s}_k) \end{bmatrix} \quad (XVI)$$

where:

$$A_{ij} = -\text{Im} \frac{1}{2\pi} \int_{(z_1)_j}^{(z_2)_j} \frac{e^{i(\theta_i - \theta_j)}}{(z_c)_i - z_0} dz_0 \quad (XVII)$$

$$= -\text{Im} \frac{e^{i(\theta_i - \theta_j)}}{2\pi} \text{Log} \frac{(z_c)_i - (z_1)_j}{(z_c)_i - (z_2)_j} \quad \text{for } 1 \leq i \leq k \text{ and } 1 \leq j \leq k \quad (XVIII)$$

For $i=j$, the influence coefficient A_{ii} can take the value $1/2$ as well as $-1/2$; as $(z_c)_i$ is considered situated on the positive side of the normal direction, it is convenient to impose $A_{ii} = 1/2$; details can be found in [1].

We notice that the appropriate choice of the singularities in relation to the boundary conditions leads to the diagonal terms $[A_{ij}]$ being preponderant and the system of equations (XVI) being well conditioned.

The resolution of the system (XVI) yields the densities of the distributed sources and vortices. Our goal is to evaluate the pressure distribution over the contour of the blade profile, it is then necessary to evaluate the tangential velocities at the different collocation points. At $(z_c)_i$ for example we can write [1,7]:

$$u_{si} = \vec{V}_0 \cdot \vec{s}_i + \int_S \mathbf{R} \left[\frac{q + i\gamma}{2\pi} \frac{e^{i(\theta_i - \theta_0)}}{(z_c)_i - z_0} dz_0 \right] \quad (XIX)$$

which can be written for $q + i\gamma = 1$; as:

$$u_{si} = \vec{V}_0 \cdot \vec{s}_i + B_{ij} s_i \quad (XX)$$

Where B_{ij} is the influence coefficient, given by :

$$B_{i,j} = R \frac{1}{2\pi} \int_{(z_1)_j}^{(z_2)_j} \frac{e^{i(\theta_i - \theta_j)}}{(z_c)_i - z_0} dz_0 \quad (XXI)$$

$$\Leftrightarrow B_{i,j} = R \frac{e^{i(\theta_i - \theta_j)}}{2\pi} \text{Log} \frac{(z_c)_i - (z_1)_j}{(z_c)_i - (z_2)_j} \quad (XXII)$$

In equation (22), when $i=j$, the expression $R \text{Log} \frac{(z_c)_i - (z_1)_j}{(z_c)_i - (z_2)_j}$ can take the values $1/2$ or $-1/2$; the value $1/2$ should be imposed.

The pressure coefficient can then be computed from:

$$C_{pi} = 1 - \frac{u_{si}^2}{V_0^2} \quad (XXIII)$$

Later on, the lift, drag and moment coefficients are computed.

4. RESULTS AND DISCUSSIONS

The numerical code developed has been executed using the airfoils FFA-W3-241 and NACA 63(2)215 represented in fig.2 and fig.3

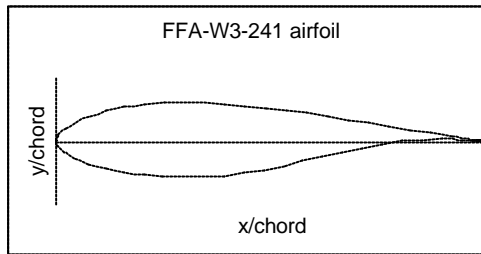


Fig.2. FFA-W3-241 airfoil

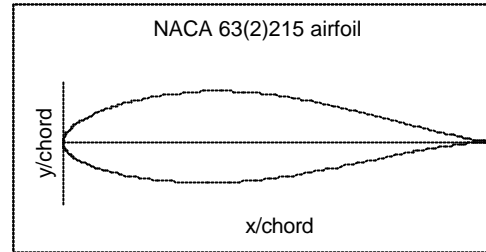


Fig.3. NACA 63(2)215 airfoil

We check the sensitivity of the numerical solution to the number of panels by comparing force results and pressure distributions with increasing number of panels. The numerical code developed uses an inviscid incompressible flow field model; the drag is negligibly small. Fig. 4 shows the drag coefficient approaching a constant value. In fact the drag is never zero because apart from viscous effects, there is also an additional form drag arising from the local variations of pressure on the airfoil surface. Fig. 5 shows the lift becoming constant as the number of panels increase. The results plotted in fig.4 and fig.5 indicate that 80 to 100 panels should be enough panels. Note that the lift and drag are presented in extremely expanded scales. The sensitivity of pressure distributions to the number of panels is also investigated. Fig.6 contains a comparison between 40 and 80 panel cases. It reveals that the stagnation pressure region on the upper surface of the leading edge is not well distinct with 40 panels. The pressure distribution at the lower surface of the airfoil just next to the lower stagnation pressure region is also not clearly resolved with 40 panels. In this case it appears that the pressure distribution is well defined with 80 panels. This is confirmed in fig.7, which shows that it is almost impossible to identify the difference between the 80 and 100 panel cases.

Having examined the convergence of the numerical solution, we investigate the agreement with experimental data.

Fig.8 compares lift from the inviscid solution obtained from the code developed with experimental data from [5]. Agreement is good at the low angles of attack where the flow is fully attached. The agreement deteriorates as the angle of attack increases, and viscous effects start to show up as a reduction of lift with increasing angle of attack, until, finally the airfoil stalls.

Fig.9 presents a comparison of the computed moment characteristics (about the quarter chord point) with experimental data. We notice here again that agreement is only good for the for low attack angles and deteriorates as separation starts to occur.

In addition to the force and moment comparisons, we need to compare the pressure distributions predicted from the numerical code with experimental data from [5]. Fig.10 and fig.11 provide two examples. The FFA-W3-241 experimental pressure distributions and the NACA 63(2)215 experimental pressure distributions are compared with the numerical predictions. The agreement is very good. The primary area of disagreement is at the trailing edge. Here viscous effects act to prevent the recovery of experimental pressure to the levels predicted by the inviscid solution[7]. The other areas of disagreement be it on the upper surface of the FFA-W3-241 airfoil or on the lower surface of the NACA 63(2)215 airfoil suggest imprecisions of the experimental attack angles and the influence of viscous effects [2].

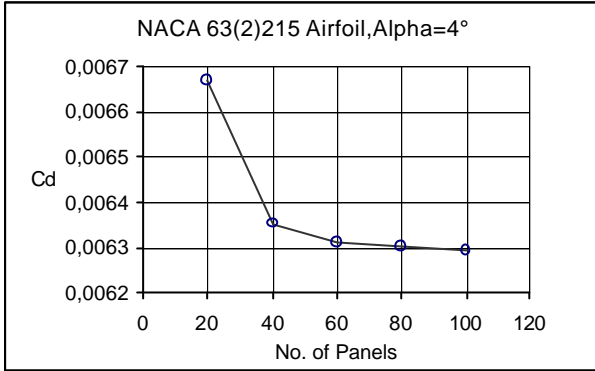


Fig.4: Change of drag with increasing number of panels

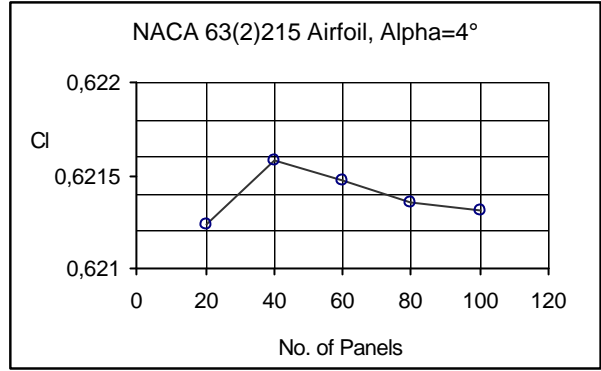


Fig.5: Change of lift with increasing number of panels

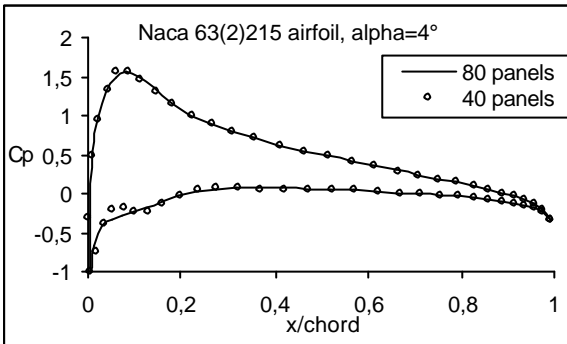


Fig.6: Pressure distribution from the numerical code , comparing results using 40 and 80 panels

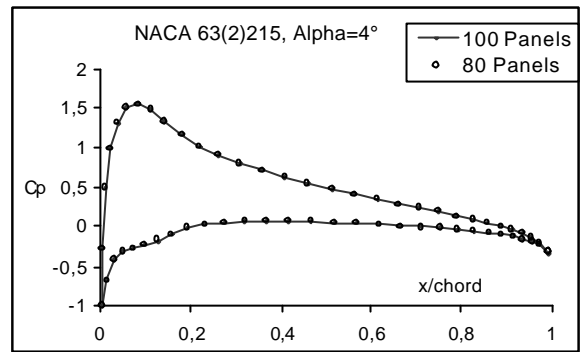


Fig.7: Pressure dis tribution from the numerical code, comparing results using 80 and 100 panels

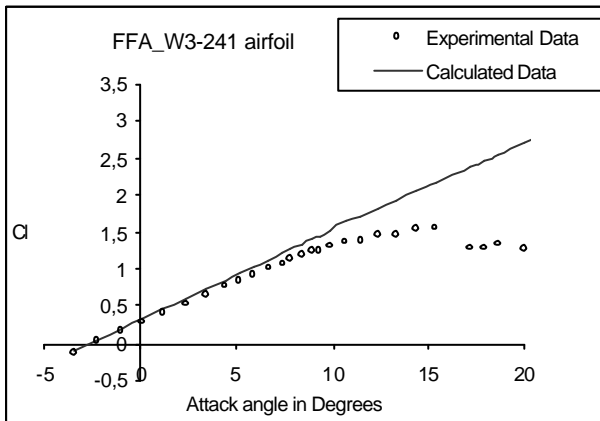


Fig.8: Comparison of Computed lift predictions with experimental data.

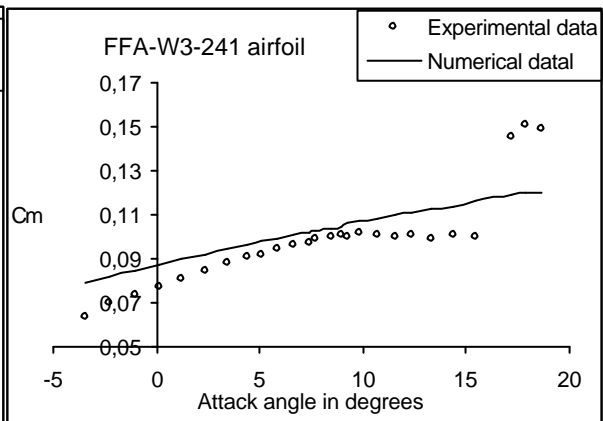


Fig.9: Comparison of Computed moment predictions with experimental data.

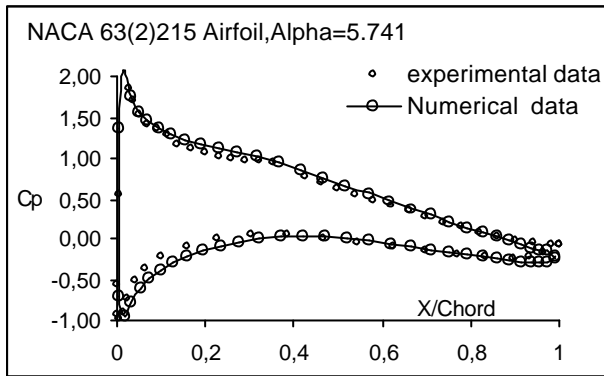


Fig.10: Comparison of Computed pressure distribution with experimental data for NACA 63(2)215 airfoil

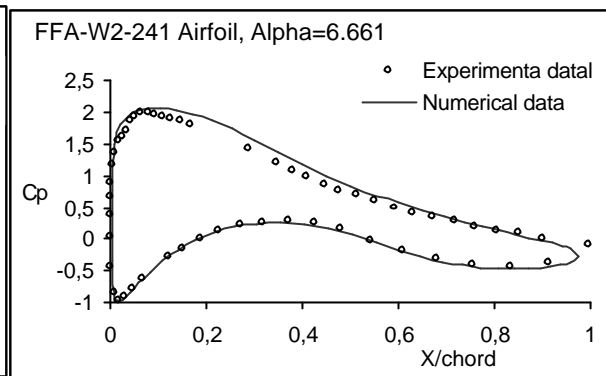


Fig.11: Comparison of Computed pressure distribution with experimental data for FFA-W3-241 airfoil

4. CONCLUSION

A 2D inviscid computational code for airfoil analysis has been developed based on the singularities method. The results obtained have shown considerable agreement with experimental data obtained from Risø National Laboratory, Roskilde, Denmark, August 2001.

In reality viscous effects are always present and the future versions of this code shall be computed to capture viscous effects.

REFERENCES

- [1] Daniel Euvrand, "Résolution Numériques des équations aux dérivées partielles", Masson 1990
- [2] F.Bertagnolio, N.Sørensen, J.Johansen and P.Fuglsang
"Wind Turbine Airfoil Catalogue", Risø-R-1280 (EN), Risø National Laboratory, Roskilde, Denmark, August 2001.
- [3] J. LUNEAU, A.BONNET, "Theories de la dynamique des fluids", Cepadues-Editions, Cepad 1989
- [4] MURRAY R. SPIEGEL: "Theory and problems of complex variables", McGRAW-HILL, 1992
- [5] P. Fuglsang, I. Antoniou, K.S. Dahl and H.A. Madsen, "Tunnel Tests of the FFA-W3-241, FFA-W3-301 and NACA 63-430 Airfoils, Risø-R-1041(EN), Risø National Laboratory, Denmark, December 1998",
- [6] T.S LUU and G. COULMY
"Design problem relating to a profile or a cascade of profiles and construction of orthogonal networks using the Riemann surfaces for the multi form singularities", Advanced Boundary Element Methods, IUTAM Symposium San Antonio, Texas, 1987.
- [7] W.H. Mason, mason@aoe.vt.edu, site: www.aoe.vt.edu
"Applied computational aerodynamics text/notes
Department of Aerospace and Ocean Engineering
Virginia Polytechnic Institute and State University"